

AD-A071 737

CORNELL UNIV ITHACA N Y SCHOOL OF ELECTRICAL ENGINEERING F/G 20/12
THE LIQUID PHASE EPITAXIAL GROWTH OF HIGH PURITY, $\text{Ga}(1-x)\text{Al}(x)\text{As}$ --ETC(U)
JUN 79 A CHANDRA, L F EASTMAN

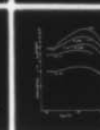
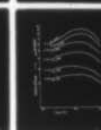
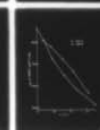
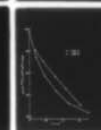
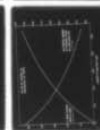
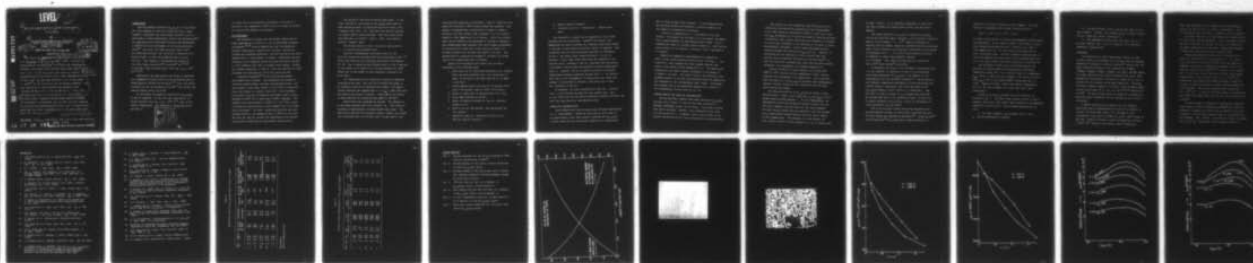
N00014-75-C-0739

UNCLASSIFIED

NL

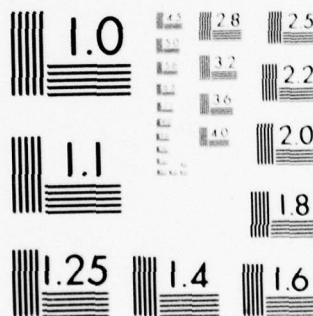
| OF |

AD
A071737



END
DATE
FILMED
8-79

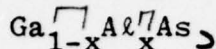
DDC



MICROCOPY RESOLUTION TEST CHART
NATIONAL BUREAU OF STANDARDS-1963-A

LEVEL II

THE LIQUID PHASE EPITAXIAL GROWTH OF HIGH PURITY



Amitabh Chandra and Lester F. Eastman
School of Electrical Engineering
Cornell University
Ithaca, N.Y. 14853

DDC
RECEIVED
JUL 26 1979
RECEIVED

N00014-75-C-0739 / Date: 22 June 1979

ABSTRACT

We report the ~~obtaining~~ ^{of} high purity in the LPE growth of $n \text{ Ga}_{1-x}\text{Al}_x\text{As}$ ($0 < x < 0.3$) at $700^\circ - 675^\circ\text{C}$. Carrier concentrations at or below $1 \times 10^{15} \text{ cm}^{-3}$ have been consistently obtained, the lowest value achieved being under $3 \times 10^{14} \text{ cm}^{-3}$ at $x = .15$. It has been shown that these low carrier concentrations do not result from a high compensation ratio. In fact, $(N_D + N_A)$ has been measured to lie in the range $1 - 2 \times 10^{15}$ for all but one of the ten samples examined. The Hall mobilities of these samples drop gradually from $\approx 100,000 \text{ cm}^2 \text{ Vsec}$ for $x = 0$ to $24,000$ for $x = .18$ at 77°K , and from $8,600$ for $x = 0$ to $5,100$ for $x = .18$ at 295°K .

We believe that a dominant shallow donor impurity (thought to be sulphur) is introduced into the melt with the aluminum. We find that the second epigrowth from a melt is significantly purer than the first, presumably due to the extra baking.

10 to The 15th power/cc

3×10 to the 14th power/cc

Key Words: $\text{Al}_x\text{Ga}_{1-x}$, high purity, LPE, III-V alloy semiconductor

79

07

16

147

098 850

APPROVED FOR PUBLIC RELEASE; DISTRIBUTION UNLIMITED

(i) start with a clean growth environment, (ii) grow at a relatively low temperature (700°C) and (iii) study the effect of x and of melt baking on the purity.

LPE PROCEDURES

The horizontal sliding boat LPE growth system used in these experiments is similar to the one described by Morkoc and Eastman,^{15,18} with an added glove box (for substrate loading) continuously flushed with nitrogen. During the loading and unloading operations, the boat and melts are hence exposed only to trace amounts of oxygen. Substrates and melt components are transferred across the glove box walls through a 1-1/2" diameter hole that is normally kept sealed. During the transfer operation, a high N_2 flow rate (50-100 cu ft/hr) minimizes the introduction of air into the glove box.

Standard procedures^{15,18} for purifying the growth environment were followed. The quartzware was cleaned in electronic grade organic solvents and deionized water, and then soaked in aqua regia before a final rinse in deionized water and drying in a laminar flow hood. After assembly, the furnace tube and the pushrods were baked under flowing hydrogen at 950°C for 4 hours and at 900°C overnight. The graphite boat was RF baked to 1200°C in a 10^{-7} Torr vacuum (followed by backfilling the vacuum chamber with ultra high purity nitrogen). The boat, loaded with gallium, was then hydrogen baked in the assembled tube at 850°C for 24 hours. The boat was used for several LPE experiments with several melts before conducting the experiments reported here.

Two series of (Ga,Al)As epilayers were grown. In the first (series F), ten layers of $\text{Ga}_{1-x}\text{Al}_x\text{As}$ were grown on semi-insulating GaAs: Gr substrates from five melts, with x ranging from .02 to .18. Each melt was used for growing two layers before being discarded. The first layer grown from each melt is called a 'type-A' layer, the second is called a 'type-B' layer.

The second series of layers (series H) were grown at $x \approx .3$, and will be discussed later.

Practical thermodynamic calculated data for the Ga-Al-As system was obtained from the calculations of Shen¹⁹, which were based on the techniques described in references 20, 21. Fig. 1 shows the equilibrium value of x as a function of the amount of Al added to a 10 gm gallium melt at 700°C. Shown also is the weight of GaAs required to saturate the Ga-Al melt.

.01" MARZ grade Al wire supplied by Materials Research Corporation was used. The thin wire allowed the weight to be carefully selected by measuring the length (1.33 mg/cm). Crystal Specialities undoped GaAs (with $\mu_{300} = 5500 \text{ cm}^2/\text{V-sec}$) was used as the source of arsenic. About 95% of the amount of GaAs required for saturation was added to the melt.

Growth melts were prepared as follows. The amounts of Al and GaAs required were first weighed out. Two pieces of aluminum of approximately the same weight were taken. The GaAs source material was standard cleaned, etched, and loaded into the growth well of the boat with a 10 gm ingot of six

nines gallium (supplied by Alusuisse). The Ga + GaAs melt was baked for 36 hours at 700°C before adding the aluminum. Both pieces of aluminum were ultrasonically cleaned in organic solvents, and then etched in HF: methanol (1:1) in a plastic beaker at room temperature for 3 minutes. After the etching step, the Al oxidation was minimized by rinsing in methanol, and transferring under methanol into the nitrogen atmosphere of the glove box, where one of the pieces was dried in a flowing stream of dry nitrogen and added to the melt. The second piece of aluminum was weighed to estimate the weight loss of the loaded piece due to etching.

Types A and B epilayers were grown from the melts according to the following steps:

1. Load first set of source-seed substrate (s-s, undoped GaAs) and main substrate (m-s, non converting S.I. GaAs) in the boat at the same time the Al is added to the melt.
2. After purging reactor with H₂ for 75 minutes (flow rate = 750 ml/min), bake at 700°C for 23 hours.
3. Bring s-s under melt to saturate melt for 1 hour.
4. Start ramp cooling (at 12°C/hr).
5. After 15 minutes of growth on the s-s, initiate growth on m-s.
6. Grow on m-s for 135 minutes, then end growth and cool reactor.
7. Unload m-s and s-s. Load new m-s and s-s for 2nd run (type B) from melt.

8. Repeat steps 2 through 6.
9. Unload m-s and s-s. Discard melt. Prepare next melt.

The necessity to reduce the air exposure of the etched aluminum was not established. Dawson²² and others⁷ have emphasized the need to prevent any aluminum oxide being formed in the melt if good quality epitaxial layers are desired. They accomplish this by using techniques described in references 22 and 7, and obtain shiny oxide-free melts. In our experience, a thin light brown oxide scum was observed on the Ga-Al-As melts, although it did not interfere with the growth of epilayers, which always had excellent surface morphologies (Fig. 2). However, the s-s's usually attained poor surface morphologies showing incomplete wetting (Fig. 3). We believe that the s-s was instrumental in wiping clean any oxide slag present at the bottom of the melt, thus providing a clean melt interface to the m-s.

As expected, the slag increased with each run. One melt (not of the F-series) was used for four growth runs. Only in the fourth run were any major morphology problems observed, and that over less than half the substrate area.

COMPOSITION DETERMINATION

Layer compositions were obtained from 5°K photoluminescence (p.l.) measurements. Radiative efficiencies were found to be significantly lower than normally observed for $\text{Ga}_{1-x}\text{Al}_x\text{As}$. A likely cause was the post-growth immersion in concentrated

HCl to dissolve small melt droplets. It was suspected that HCl affected surface stoichiometry to greatly enhance the non radiative recombination processes.

Values of x measured by p.l. correspond to the layer surface. We studied the uniformity of x with depth for sample F-18, using Secondary Ion Mass Spectroscopy (SIMS). The Al response was found to increase almost linearly by ~12% from the layer surface to the substrate interface, over a thickness of 9.2 microns.

Results of composition measurements are compared in Table A with values predicted theoretically from Fig. 1. For simplicity, layer compositions were assumed constant and equal to the surface values measured by p.l. The theoretical compositions for type A layers correspond to the weight of Al added to the melt. For type B layers, the lowering of the aluminum content of the melt was estimated from the composition and thickness of the corresponding type A layer. Good agreement between theory and experiment supports the validity of the thermodynamic calculations of ref. 19.

CARRIER DENSITY AND MOBILITY DETERMINATION

Van der Pauw Hall samples were made from each $\text{Ga}_{1-x}\text{Al}_x\text{As}$ epilayer with x below .2, and tin dots were alloyed in a hydrogen atmosphere using a strip heater. Good ohmic contacts were easily obtained. However, this technique did not work for the series of $x \approx .3$ samples, with a native oxide on the surface preventing the tin from alloying with the semiconductor.

The results of room temperature and 77°K electron concentrations and mobilities determined by Hall measurements at $B = 2000$ gauss are presented in Table B, which also lists the n_{295} determined by C-V profiling using Au Schottky barriers. "Uncorrected" Hall carrier densities were obtained by assuming the electrical thickness of the epilayers to be equal to their metallurgical thickness. Fairly large discrepancies were observed between the uncorrected n_{Hall} and n_{CV} . However, by accounting for the depletion of free carriers near the surface and the substrate interface of the epilayers²³, so that the electrical thickness was lower than the metallurgical thickness, this discrepancy was reduced significantly.

Carrier freezeout in these samples, on cooling from 295°K to 77°K, was well within experimental error, and was therefore not considered to be significant. This indicated that the donors in the $\text{Ga}_{1-x}\text{Al}_x\text{As}$ epilayers were predominantly shallow, thereby ruling out the possibility that the main donor species was oxygen.

The electron mobility of $\text{Ga}_{1-x}\text{Al}_x\text{As}$ was found to drop rapidly with x . Figs. 4 and 5 show the μ_{77} and μ_{295} of the F series layers plotted against x . At both temperatures, the experimental points fall along two distinct curves, one for the type A samples, and the other for the type B samples. For each A-B pair grown from the same melt, the type B sample has a significantly higher mobility than the type A sample, at both temperatures. The decrease in x can account for only a small fraction of the increase in μ , as is clearly seen

in Figs. 4 and 5. It is therefore reasonable to infer that the type B samples are significantly purer than the type A samples.

The large reduction of μ_{77} with x cannot be accounted for by the relatively small increase in the electronic effective mass m^* in the range $0 < x < .2$.²⁴ Hence the decrease in mobility must be largely caused by increased electron scattering. Upper valley transport and intervalley scattering at low fields are negligible for $x < .2$ at 77°K ,⁹ while phonon scattering is expected to remain approximately constant as x increases. That leaves ionized impurity scattering and alloy²⁵/space-charge²⁶ scattering.

To determine the cause of the increase in scattering with x in our samples, we undertook a study of the intravalley scattering mechanisms in $\text{Ga}_{1-x}\text{Al}_x\text{As}$. The details of this investigation will be described elsewhere.²⁷ Use was made of the different temperature dependence of alloy scattering and ionized impurity scattering. Hall data was taken on the $\text{Ga}_{1-x}\text{Al}_x\text{As}$ samples at 25 to 110°K at $B = 2000$ gauss. Figs. 6(a) and (b) show the plots of μ_H vs temperature measured. By fitting this data to our theoretical model, we were able to obtain estimates of N_A and N_D , as well as information on alloy scattering for each sample.

The alloy and space charge scattering mechanisms were grouped together because two scattering cross-sections have the same energy and temperature dependence²⁸. Kaneko et al.²⁸ and Stringfellow²⁹ have found space charge scattering to

dominate over alloy scattering in their samples. The same empirical x-dependent space charge scattering factor

$$N_s Q = 5 \times 10^3 + 6.3 \times 10^5 x \text{ (cm}^{-1}\text{)} \quad (1)$$

is used by both authors to obtain good agreement between theory and experiment. In our layers, however, the extent of alloy/space-charge scattering was only a fraction (7 to 15%) of that suggested by Eq. (1), and could be accounted for by alloy scattering alone. We could therefore conclude that our (Ga,Al)As samples were high quality with a minimal density if any of the space-charge scatterers described in reference 26.

The increase of phonon and alloy scattering and the decrease of ionized impurity scattering with increasing temperature causes the μ vs T curves to peak at a temperature T_{\max} , which is lower for purer samples. The curves in Fig. 6 show T_{\max} to be in the range 50-60°K, indicating that (i) these samples are pure, rather than heavily compensated, and (ii) the type B samples are purer than their type A counterparts.

Values of N_A and N_D obtained from this analysis are plotted in Fig. 7. The heavy lines connect values of type A samples, while thin lines connect type A points to corresponding (same melt) type B points. The following observations are clear:

1. For type A samples, N_D increases with x, while N_A remains approximately constant.

2. For each A-B pair, both N_A and N_D are lower for the type B sample. However, the decrease in N_D is larger, resulting in a lower net carrier concentration.

3. The compensation ration $(N_D + N_A)/(N_D - N_A)$ is ≈ 2 for most samples, and < 4 for all samples, as is typically observed in undoped GaAs.

DISCUSSION

An explanation of these experimental results is that a donor species is introduced into the melt with the aluminum. Examining the supplier's material analysis³⁰ reveals that the major impurities present in the aluminum are O(30ppm), C(20ppm), N(5ppm), S(5ppm), H(3ppm), Ca(.3ppm), and Mg(.26ppm). All other impurities have quoted concentrations below .1ppm. Segregation coefficients of Sn and Si in GaAs are too low to account for the increase in the donor densities. The group VI donors, however, namely S, Se and Te, have estimated segregation coefficients (K) of ~45, 14, and 4.5^{31,32} respectively at 700°C. We have already ruled out oxygen as a possibility. Thus the donor introduced with the aluminum is most likely to be sulphur.

A simple calculation for sample F-14 (for example) shows that there is approximately one atom of Al present in the melt for every 3870 atoms of Ga, and 5ppm S in Al corresponds to one atom of sulphur for every 7.8×10^8 atoms of gallium. Using $K = 45$ gives a donor incorporation of about $1.3 \times 10^{15} \text{ cm}^{-3}$, which is the correct order of magnitude.

(The close agreement of this number with the experimental value of N_D for F-14 is, of course a coincidence). Thus our contention that the donor is sulphur is quite plausible.

The donor density in the melt drops quite significantly for the second (type B) epigrowth. Donor incorporation into the type A epilayer can account for only a 1% reduction of the donor concentration in the melt. Some other mechanism of donor loss from the melt must therefore exist.

Further experiments (H-series) were conducted in an effort to obtain purity in $\text{Ga}_{1-x}\text{Al}_x\text{As}$ at $x = .3$. With a total bake time of 40 hours at 700°C after the addition of aluminum, the carrier concentration obtained in the first epilayer (type A) was $2.5 \times 10^{15} \text{ cm}^{-3}$ ($\pm 25\%$). For a second melt, a total bake time of 92 hours at 700°C after adding aluminum gave a first epilayer with $n = 1.4 \times 10^{15} \text{ cm}^{-3}$. A third melt was baked after adding aluminum at 900°C for 13 hours followed by 92 hours at 700°C , before growing the first epilayer. The carrier concentration obtained was $1.1 \times 10^{15} \text{ cm}^{-3}$. In each of the three cases, the substrates were loaded and baked along with the melt for 22 hours prior to growth.

In their study of Cr doping of high purity n GaAs epilayers grown at 700°C , Woodard and Eastman³² have used the technique of baking the Ga-As-Cr melt at 900°C for 15 hours to remove a volatile donor impurity that is introduced with the chromium. This, however, increases the silicon contamination of the melt, which must then be baked at 700°C to

lower the silicon concentration. They have shown that about 96 hours of baking at 700°C brings the total Si incorporation to $\leq 2 \times 10^{14} \text{ cm}^{-3}$. Our observations on growth from Ga-Al-As melts show the positive effect of such baking techniques on layer purity, but also indicate that the purification process is slower than in the Ga-As-Cr case. This is probably because the oxide on the melt prevents the sulphur from escaping, except through cracks.

We suspect that the oxide slag itself is responsible for gettering the impurities from the melt. We speculate that each time the boat is taken out of the furnace tube into the glove box, trace amounts of oxygen are trapped between the surfaces of the boat. On baking, some oxygen diffuses to the melt forming aluminum oxide which collects at the melt's surfaces. The extent of impurity gettering by the slag is limited by the amount (of slag) produced; hence the correlation between the number of previous epi-runs from a melt and the layer purity.

In conclusion, we have obtained the highest purity in $\text{Ga}_{1-x}\text{Al}_x\text{As}$ ($x < .3$) reported so far to our knowledge by growing at 700°C in a clean environment, and by following baking procedures after adding aluminum to the melt. These layers were grown in a reactor which gives a μ_{77} of only $100,000 \text{ cm}^2/\text{Vsec}$ for undoped GaAs, compared with $150,000 - 170,000 \text{ cm}^2/\text{Vsec}$ obtained in the best systems in our laboratory, indicating room for further improvement. Also, the possibility exists of using Woodard's³³ $900^{\circ}\text{C} + 700^{\circ}\text{C}$ baking

technique to obtain even higher purity, provided oxide slag formation can be prevented by using Dawson's methods²².

ACKNOWLEDGEMENTS

We are indebted to Dr. Ron Nelson of Bell Labs for the photoluminescence measurements, to Dr. David Hodul of Cornell for the SIMS profiles, and to our colleague Dr. Colin Wood for his critical appraisal and helpful comments with the manuscript. This work was supported by the Office of Naval Research under Contract # N00014-75-C-0739.

REFERENCES

1. J.F. Black and F.M. Ku, J. Electrochem Soc., 113, 249, (1966).
2. H. Rupprecht, J.M. Woodall and G.D. Pettit, Appl. Phys. Lett., 11, p. 81, (1967).
3. K.J. Linden, J. Appl. Phys., 40, p. 2325, (1969).
4. Zh. I. Alferov, V.M. Andreyev, V.I. Korol'kov, E.L. Portnoi and D.N. Tret'yakov, Sov. Phys. Semicond., 2, p. 1289, (1969).
5. H. Kressel and H. Nelson, RCA Rev., 30, p. 106, (1969).
6. I. Hayashi, M.B. Panish and P.W. Foy, IEEE J. Quantum Electronics, 5, p. 211, (1969).
7. J.M. Woodall and H.J. Hovel, J. Cryst. Growth, 39, p. 108, (1977).
8. M.S. Saidov, V.V. Nikitin, B. Sadaev, G.N. Kovardakova and A.S. Saidov, Sov. Phys. Semicond., 10, p. 1038, (1976).
9. T. Sugeta, A. Majerfeld, A.K. Saxena, P.N. Robson and G. Hill, 6th Biennial Cornell Elec. Engineering Conf., p. 45, (1977).
10. D.V. Lang and R.A. Logan, Appl. Phys. Lett., 31, p. 683, (1977).
11. C.M. Garner, Y.D. Shen, C.Y. Su, G.L. Pearson and W.E. Spicer, J. Vac. Sci. Technol., 15, p. 1480, (1978).
12. D. Cheung, Ph. D. Dissertation, Stanford University, (1975).
13. C.S. Kang and P.E. Green, Appl. Phys. Lett., 11, p. 171, (1967).
14. H.G.B. Hicks and D.F. Manley, Solid State Commun., 7, p. 1463, (1969).
15. H. Morkoc and L.F. Eastman, J. Cryst. Growth, 36, p. 109, (1976).
16. A. Chandra and L.F. Eastman, Electronic Lett., 15, 90 (1979).
17. A. Chandra and L.F. Eastman, "The Use of a $\text{Ga}_{1-x}\text{Al}_x\text{As-GaAs}$ Interface for Electron Confinement in Low Noise FETs", presented at the Workshop on Compound Semiconductor Materials and Devices, San Francisco, Feb. 1978.

18. H. Morkoc and L.F. Eastman, J. Electrochem Soc., 123, p. 906, (1976).
19. Y.D. Shen, Stanford Univ. Results communicated by G.L. Pearson.
20. M. Ilegems and G.L. Pearson, Proc. 2nd Intl. Symp. on GaAs, 1968, p. 3.
21. M.B. Panish and M. Ilegems, Progress in Solid State Chemistry, Vol. 7, p. 39.
22. L.R. Dawson, J. Cryst. Growth, 27, p. 86, (1974).
23. A. Chandra, C.E.C. Wood, D. Woodard and L.F. Eastman "Surface and Interface Depletion Corrections to Free Carrier Density Determinations by Hall Measurements", Solid State Electronics, to be published.
24. R. Dingle, R.A. Logan, and J.R. Arthur, Jr., Proc. 6th Intl. Symp. on GaAs and Related Compounds, Edinburgh, p. 210, (1976).
25. J.W. Harrison and J.R. Hauser, Phys. Rev., B13, p. 5347, (1976)
26. L.R. Weisberg, J. Appl. Phys., 33, p. 1817, (1962).
27. A. Chandra and L.F. Eastman, A Study of Alloy Scattering in High Purity $\text{Ga}_{1-x}\text{Al}_x\text{As}$ ", in preparation.
28. K. Kaneko, M. Ayabe and N. Watanabe, Proc. 6th Intl. Symp. on GaAs and Related Compounds, Edinburgh, p. 216. (1976).
29. G. B. Stringfellow, "Electron Mobility in $\text{A}_x\text{Ga}_{1-x}\text{As}$ ", J. Appl. Phys., to be published
30. Materials for Research Catalogue, Materials Research Corporation, Route 303, Orangeburg, New York 10962.
31. C.S. Kang and P.E. Greene, Proc. 2nd Intl. Symp. on GaAs, 1968, p. 18.
32. H.G.B. Hicks and P.D. Greene, Private Communication.
33. D. Woodard, Ph.D. Dissertation, Cornell Univ., (1979).

Table A

Composition Data on $\text{Ga}_{1-x}\text{Al}_x\text{As}$ Layers Grown at 700°C

Melt #	Sample #	wt of Al in 10gm Ga (mg)	Thickness (microns)	x_{theory} (%)	wt of Al depleted (mg)	Photolum (5 ⁰ K) peak energy (eV)	x from photoluminescence (%)
I	A F-10	.25	11.1	2.1	.03*	1.545	2.0
	B F-11	.22*	11.1	1.75		1.541	1.75
II	A F-12	.56	12.0	5.1	.06*	1.581	4.6
	B F-13	.48*	13.9	4.3		1.577	4.2
III	A F-14	1.0	11.4	8.8	.13*	1.632	8.2
	B F-15	.87*	13.0	7.7		1.625(uncertain)	7.8
IV	A F-16	1.5	11.1	12.6	.185*	1.682	11.8
	B F-17	1.31*	10.3	11.3		1.670	11.0
V	A F-18	2.13	9.3	17.1	.21*	1.744	17.7
	B F-19	1.92*	9.5	15.6		1.726	15.4

* Estimated

† Best estimated value

Table B
Carrier Density Measurements on $\text{Ga}_{1-x}\text{Al}_x\text{As}$ Samples

Melt Type	Run #	X% (approx)	μ_{77} (cm^2/Vsec)	μ_{295} (cm^2/Vsec)	n_{Hall} Uncorrected ($\times 10^{14} \text{ cm}^{-3}$)	n_{CV} ($\times 10^{14} \text{ cm}^{-3}$)	n_{Hall} Corrected ($\times 10^{14} \text{ cm}^{-3}$)
I	A F10	2.0	74200	8080	3.2	6.2	4.6
	B F11	1.75	80950	8070	4.5	7.2	6.0
II	A F12	4.6	57550	7225	5.9	7.8	7.4
	B F13	4.2	70450	7770	4.3	7.6	5.3
III	A F14	8.2	43000	6500	5.7	7.4	7.2
	B F15	7.8	56600	7190	4.7	5.9	6.0
IV	A F16	11.8	32200	5840	7.6	8.4	9.0
	B F17	11.0	45650	6655	3.5	6.8	4.6
V	A F18	17.7	23850	5130	8.0	9.8	9.6
	B F19	15.4	30650	5680	1.7	2.7	2.6

FIGURE CAPTIONS

- Fig. 1. Solidus isotherms for the Ga-Al-As system at 700°C, from the calculations of Shen¹⁹.
- Fig. 2. Photomicrograph of the typical surface morphology of grown $\text{Ga}_{1-x}\text{Al}_x\text{As}$ layers.
- Fig. 3. Photomicrograph of the source-seed after a growth run, showing incomplete wetting presumably caused by oxide under the melt.
- Fig. 4. 77°K Hall mobility data (at 2 KGauss) of $\text{Ga}_{1-x}\text{Al}_x\text{As}$ layers, plotted against x.
- Fig. 5. Room temperature Hall mobility data (at 2 KGauss) of $\text{Ga}_{1-x}\text{Al}_x\text{As}$ layers, plotted against x.
- Fig. 6. (a),(b) Temperature variation of Hall mobility (at 2 KGauss) for the $\text{Ga}_{1-x}\text{Al}_x\text{As}$ layers.
- Fig. 7. Donor and acceptor densities vs x for type A and type B $\text{Ga}_{1-x}\text{Al}_x\text{As}$ layers.

